Linewidth Tolerance for THz Communication Systems Using Phase Estimation Algorithm

Luis Gonzalez-Guerrero, Haymen Shams, Martyn J. Fice, Alwyn J. Seeds, Cyril C. Renaud
Department of Electronic and Electrical Engineering,
University College London,
London, UK
* luis.guerrero.14@ucl.ac.uk

Frédéric van Dijk
III-V Lab, a joint Laboratory of "Alcatel Lucent Bell Labs", "Thales Research & Technology" and "CEA-LETI",
Palaiseau, France

***Abstract*—This paper presents the impact of signal linewidth on photonic THz wireless systems using phase estimation (PE) algorithms at the receiver. The penalty associated with signal linewidth, as well as the optical linewidth requirements for systems using free-running lasers are evaluated using extensive Monte Carlo simulations for different modulation formats. The BER performance and power penalty induced by signal linewidth are also measured experimentally by varying the linewidth of the local oscillator laser. Simulation and experimental results show similar penalty trends. Differences between them are likely to be due to impairments not considered in the simulations and the THz signal linewidth being bigger than the sum of the optical linewidths of the two free-running lasers used in the experiment.**

Keywords— Photonic THz generation, optical heterodyning, digital coherent detection; high-speed wireless; fibre wireless; radio-over-fibre.

I. INTRODUCTION

The lower THz band (100 GHz – 450 GHz) has already shown great promise to increase the capacity of wireless networks and overcome the spectrum congestion at lower frequency bands [1]. Given the limited propagation distance at THz frequencies (due to free-space path loss and atmospheric attenuation) and their directional nature, the distribution of THz signals over an optical fiber is a very attractive solution to extend the range of such systems. In this scheme optical fibers are used to connect the central station (CS) to distributed remote antennas units (RAUs) where the THz signal is emitted into free space. The signal is then received by a mobile or fixed unit. Because of the limited range of THz systems, the remote THz antenna units will need to be low cost, as large numbers will be required.

The photonic multichannel configuration for the THz distribution that we envisage in this paper is shown in Fig. 1. Several optical carriers are generated and modulated at the CS. An unmodulated line is used as the local oscillator (LO) in the photomixing process, which takes place in a fast photodetector at the antenna unit. After free-space propagation, the THz signal generated at the photodetector is received by a wireless unit, where it is down-converted to baseband and demodulated. Due to uncorrelated phase noise and relative frequency fluctuations between the optical carriers and the LO, the THz signal will exhibit both phase noise and frequency fluctuations. If coherent detection is used at the receiver (which will be required in long range transmissions and links using high-order modulation formats) these impairments can affect the BER performance of the system.

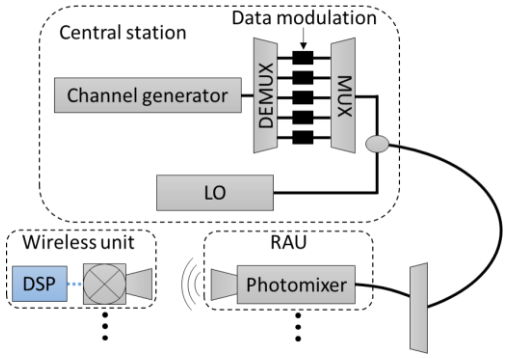

Fig. 1. Schematic of photonic multichannel THz distribution. DEMUX and MUX are optical demultiplexer and multiplexer, respectively, and RAU is remote antenna unit.

Phase noise can be combatted both at the transmitter side and the receiver side. Solutions at the transmitter side rely on the use of optical frequency comb generator (OFCG) lines for both the optical carrier and LO [2], and the implementation of phase stabilization techniques to achieve high purity signals [3]. On the other hand, digital signal processing (DSP) techniques from optical coherent communications can be used to compensate for phase noise at the receiver after electrical down conversion to an intermediate frequency (IF) [4]. In particular, phase estimation (PE) algorithms provide simple and efficient means for removing the phase noise in multi-level signals like quadrature phase shift keying (QPSK) or 16-quadrature amplitude modulation (QAM). Although DSP will increase the latency of THz systems and its real-time implementation is challenging at high symbol rates, its use in systems with high-order modulation formats will be necessary even if phase correlated optical carriers are used at the transmitter [5]. This is due to phase instabilities caused by temperature changes and unmatched

transmission paths between the modulated signal and unmodulated carrier.

In optical networks, PE algorithms relax the spectral purity requirements of the transmitter and enable the use of free-running lasers, which greatly simplifies the system design. This advantage is also to be expected in THz communication systems using these algorithms. However, their implementation leads to a small penalty with respect to the theoretical achievable performances. The knowledge of the level of penalty is key to making an accurate estimation of the link budget, which will ultimately determine the performance of the system under consideration.

In this paper we investigate through extensive Monte Carlo (MC) simulations the impact that the signal linewidth has on the BER performance of a photonic THz wireless system. The total THz linewidth, as well as the laser linewidth requirement for two free-running lasers, are determined for different modulation formats (QPSK, 16- and 64-QAM) at a BER of 10^{-3}. The power penalties induced do to laser linewidth are also investigated experimentally through BER measurements. The penalty obtained experimentally is bigger than that from simulations. We believe this may be caused due to impairments which were not considered in the MC simulations (limited to phase noise and white Gaussian noise) and the THz signal linewidth being bigger than the sum of the optical linewidths of the two free-running lasers used in the experiment.

II. Simulations

A. *Estimation of the penalty for different THz linewidth-symbol duration products*

For this work our simulations were limited to square QAM constellations (QPSK, 16-QAM and 64-QAM) since their generation requires a simpler optical transmitter design compared to other high-order modulation formats like phase shift keying (PSK) or star QAM. There are a number of PE algorithms readily available from optical communications that can successfully recover the phase information in this type of signals [6]. Two of the most popular ones are the so called blind phase search (BPS) [7] and the Viterbi-Viterbi algorithm with block averaging (also referred to as *M*-th power block algorithm) [8]. Although both of them have similar performance for QPSK, the BPS algorithm yields slightly better results for higher modulation formats because, unlike the *M*-th power block scheme, it uses all the received samples to make an estimation of the phase noise. Some techniques have been proposed to improve the performance of the *M*-th power algorithm in this regard [9]. However, these techniques, together with the BPS algorithm, have increased computational complexity if compared to the *M*-th power algorithm. For this reason, we choose to perform our simulations and experiments with the latter technique.

The samples at the input of the PE algorithm can be described as:

$$m(k)\exp\left(j\theta(k)\right) + n(k), \qquad (1)$$

where $m(k)$ is the complex data symbol, $\theta(k)$ is the phase noise, $n(k)$ is the complex additive, white, Gaussian noise (AWGN) and k is the symbol number. The power spectrum of the generated THz signal from photomixing was modeled using a Gaussian-distributed phase deviation over the symbol period (T_s) with zero mean and variance ${\sigma_p}^2 = 2\pi\Delta\upsilon T_s$, where $\Delta\upsilon$ is the full-width half maximum linewidth of the THz signal. The THz linewidth $\Delta\upsilon$ may be assumed to be the sum of the optical linewidths if two free-running lasers are used. Both inter-symbol interference (ISI) and frequency offset are assumed to be fully removed by previous DSP blocks and the resolution of the analog-to-digital converter is assumed to be sufficient to yield the best performance.

The *M*-th power block algorithm is based on raising the incoming samples to the 4-th power (in case of QAM constellation diagrams) to wipe off the phase signal. Then, the phase noise is estimated by averaging over a certain number of samples. The optimum number of samples for best performance was calculated analytically for QPSK [10], while the optimum number of samples for 16- and 64-QAM was found numerically. To combat the four-fold ambiguity associated with square QAM constellations, the data are differentially encoded at the transmitter. However, differential encoding is only applied to the first two bits of each symbol in order to minimize the penalty associated with differential decoding [11]. For the 64-QAM simulations, only the symbols on the inner and outer circle were used to calculate the phase error estimate. The power penalty vs. the ratio between the THz linewidth and symbol rate ($\Delta\upsilon \cdot T_s$) for QPSK, 16-QAM and 64-QAM is shown in Fig. 2. The power penalty was calculated from the difference of signal-to-noise ratio (SNR) per bit between the simulated curves and the theoretical value with no phase noise and no differential decoding at a BER of 10^{-3}. As it is expected, the penalty increases with both the THz linewidth and the number of constellation points of the modulation format. Therefore, the SNR of a system limits the maximum linewidth that the system can tolerate for a given BER performance. In Table 1, the THz linewidth for accepting a receiver penalty of 2 dB at a BER of 10^{-3} and a symbol rate of 10 Gbaud is summarized for each modulation format. The optical linewidth requirement if two free-running lasers (with the same linewidth) are used is also shown.

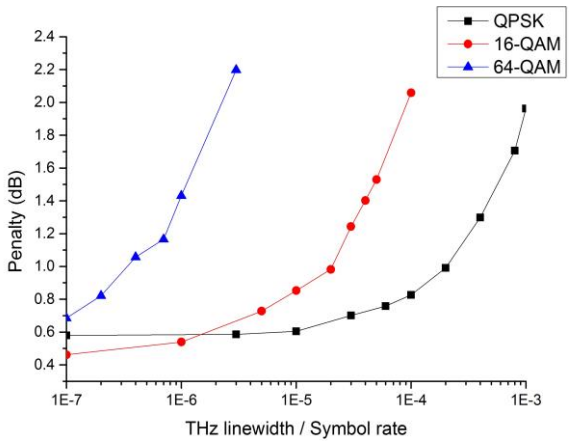

Fig. 2. Penalty at BER of 10^{-3} vs. THz linewidth-symbol duration product, $\Delta\upsilon \cdot T_s$.

TABLE I. THZ LINEWIDTH REQUIREMENTS FOR A RECEIVER PENALTY OF 2DB @ BER OF 10^{-3}

	QPSK	16-QAM	64-QAM
THz linewidth/ Symbol rate	1E-3	9.4E-5	2.5E-6
THz linewidth @ 10 Gbaud	10 MHz	940 kHz	25 kHz
Linewidth per laser	5 MHz	450 kHz	12.5 kHz

As can be seen from Table 1, the linewidth requirement for QPSK is quite relaxed, and can be met with off-shelf diode lasers. As it is expected, 16-QAM requires higher spectral purity signals, with optical linewidths in the range of hundreds of kHz. However, integrated, free-running, dual-mode lasers for THz generation exhibiting linewidths below 200 kHz have already been reported [12]. For 64-QAM, the laser phase noise becomes a critical parameter, requiring very narrow lasers that may not be commercially available. These simulations confirm that THz systems using DSP and typical commercial lasers at modulation formats up to 16 QAM would not need stabilization techniques at the transmitter side, thus leading to more flexible architectures. Even more relaxed linewidth requirements can be obtained with more complex PE algorithms [7]. However, considering the wireless unit in Fig. 1 is likely to be a mobile device, the computational effort of the algorithm will be a critical parameter that will need to be minimized. This is the reason we chose to perform the simulations and experiment with the well-established Viterbi-Viterbi algorithm.

To illustrate the effect of the penalty associated with PE-algorithms we have calculated the link budget of a THz system under different values of linewidths and source powers. The carrier frequency was chosen to be 250 GHz and the data was modulated at a speed of 10 Gbaud in the QPSK format. Both the receiver and transmitting antenna used in the calculation have a gain of 25 dBi. Additive white Gaussian noise includes the contributions of both shot and thermal noise. No amplifiers are considered. The effect of laser linewidth is included through:

$$SNR_{system}(dB) - Ref_{QPSK}(dB) = Penalty(dB) \quad (2)$$

The results are shown in Fig. 3.

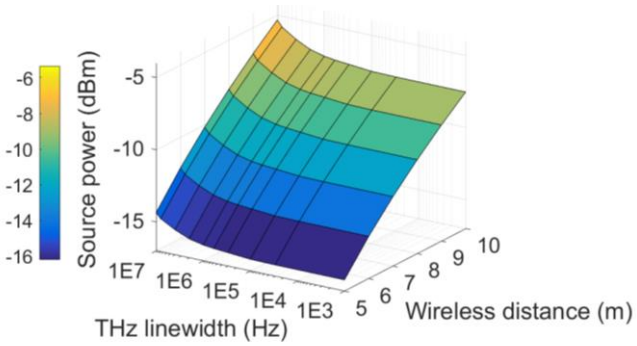

Fig. 3. Required source power vs linewidth and wireless distance

III. EXPERIMENTAL RESULTS

A. Procedure

The experimental setup used to investigate the impact of signal linewidth on a THz system is shown in Fig. 4.

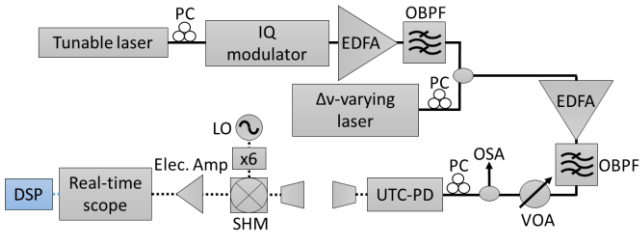

Fig. 4. Block diagram for the THz signal experiment. PC: polarization controller, OBPF: optical band pass filter, UTC-PD: uni-travelling carrier photodiode, EDFA: erbium-doped fiber amplifier, VOA: variable optical attenuator.

Since free-running lasers were used for all transmissions, the linewidth of the resulting THz signal was assumed to be equal to the sum of the optical carrier and LO linewidths. In order to achieve different THz linewidths, the linewidth of the optical LO, a standard packaged butterfly DFB laser, was varied through current injection. The laser used as optical carrier was a tunable external cavity laser with a linewidth of 70 kHz. The linewidth of the DFB laser was evaluated using the self-heterodyne technique with 5 km fiber delay [13]. Fig. 5 shows the value of both linewidths (carrier and LO) summed together versus the DFB bias current. Red stars are the linewidth points selected for the BER measurements. The inset in Fig. 5 shows the electrical spectrum of the self-heterodyne beat note and the correspondent Lorentzian fit.

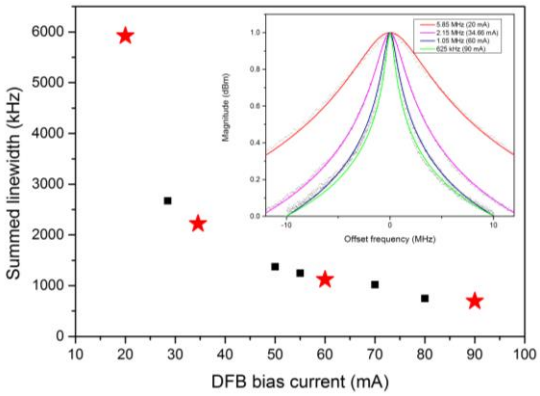

Fig. 5. Summed linewidth verus DFB laser bias (red star-shaped points represent lnewidths used in the experiment). Inset: Lorentzian fit for each of the resultant DFB line-shapes.

The wireless distance used in the experiments was kept to a minimum (around 2 cm) to compensate for the low output of the uni-travelling carrier photodiode (UTC-PD), which can be estimated to be around -30 dBm [4]. The carrier frequency was chosen to be 250 GHz as this band (220 GHz - 320 GHz) is a band of interest and offers a large transmission window (100 GHz) with no molecular absorption lines. The BER measurements were done for a 10 Gbaud QPSK modulated signal. Different values of SNR were obtained by varying the

attenuation value of the VOA. The SNR was calculated after offline DSP. The value of the noise power was measured when no optical power was transmitted through the link.

B. Results and discussions

In Fig. 6, the BER curves versus SNR for each THz linewidth as well as the penalty associated with each of them is shown.

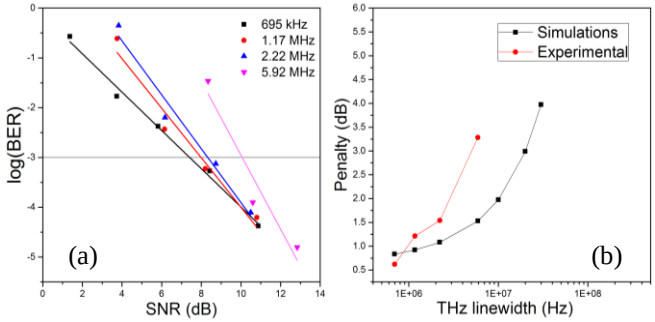

Fig. 6. (a) BER curves for 10 GBaud QPSK at different linewidths; (b) the penalty for each linewidth.

As we can see from Fig. 6 (a), it is evident that, as expected, the phase noise is having an impact on the performance of the system; it clearly shows that an increased linewidth brings a penalty and degrades the BER performance of the system. However, the slope of the BER curves appear to decrease with increased optical linewidth. This is not expected since the effect of linewidth on the system performance is expected to become more apparent at higher signal-to-noise ratios where phase noise dominates over the Gaussian noise. This is expected to be an artifact from the DSP due to a failure in finding the optimal block length in PE algorithm for each measurement point. In Fig. 6 (b), we can also notice that the experimental penalty is a bit higher than that from our simulations. This is probably due to the fact that our simulation was limited to the effect of phase noise only and no other impairments. Another possible reason may be that the actual THz linewidth of the generated signal is bigger than the optical summed linewidth. This fact has already been reported in some experiments [14]. A more accurate value of the linewidth of the THz signal could be obtained by measuring the resultant beat note in a spectrum analyzer after heterodyning the two optical modes. However, this is challenging due to the high frequency fluctuations exhibited by a beat note from two free-running lasers.

IV. Conclusions

The laser linewidth requirements were evaluated for THz wireless systems using the 4-th power digital phase estimation algorithm. The results obtained from MC simulations show the required THz linewidth for accepting a penalty of 2 dB at a BER of 10^{-3} is 5 MHz, 450 kHz, and 12.5 kHz for QPSK, 16 – and 64 –QAM, respectively. The simulation results for QPSK were also assessed experimentally. As expected, the measurements showed an increase of the penalty with THz linewidth that followed a similar trend to that calculated through simulations. The higher penalty obtained experimentally may be attributed to impairments not taken into account in the simulations and a THz signal linewidth bigger than the sum of optical linewidths.

Acknowledgment

This work was supported by the Engineering and Physical Sciences Research Council programme grant Coherent Terahertz Systems (COTS) (EP/J017671/1), and by the European Commission through the European project iPHOS (grant agreement no: 257539).

References

[1] A. J. Seeds, H. Shams, M. J. Fice, and C. C. Renaud, "TeraHertz Photonics for Wireless Communications," *J. Light. Technol.*, vol. 33, no. 3, pp. 579–587, 2015.

[2] H. Shams, T. Shao, M. J. Fice, P. M. Anandarajah, C. C. Renaud, F. Van Dijk, L. P. Barry, and A. J. Seeds, "100 Gb/s Multicarrier THz Wireless Transmission System With High Frequency Stability Based on A Gain-Switched Laser Comb Source," *IEEE Photonics J.*, vol. 7, no. 3, pp. 1–11, Jun. 2015.

[3] Y. Yoshimizu, S. Hisatake, S. Kuwano, J. Terada, N. Yoshimoto, and T. Nagatsuma, "Wireless transmission using coherent terahertz wave with phase stabilization," *IEICE Electron. Express*, vol. 10, no. 18, pp. 1–8, 2013.

[4] H. Shams, M. J. Fice, L. Gonzalez-Guerrero, C. C. Renaud, F. van Dijk, and A. J. Seeds, "Sub-THz Wireless over Fibre for Frequency Band 220 GHz- 280 GHz," *J. Light. Technol.*, pp. 1–1, 2016.

[5] T. Shao, H. Shams, P. M. Anandarajah, M. J. Fice, C. C. Renaud, F. Van Dijk, A. J. Seeds, and L. P. Barry, "Phase Noise Investigation of multicarrier Sub-THz Wireless Transmission System Based on an Injection-Locked Gain-Switched Laser," *IEEE Trans. Terahertz Sci. Technol.*, vol. 5, no. 4, pp. 590–597, 2015.

[6] X. Zhou, "An improved feed-forward carrier recovery algorithm for coherent receivers with M-QAM modulation format," *IEEE Photonics Technol. Lett.*, vol. 22, no. 14, pp. 1051–1053, 2010.

[7] T. Pfau, S. Hoffmann, and R. Noé, "Hardware-efficient coherent digital receiver concept with feedforward carrier recovery for M-QAM constellations," *J. Light. Technol.*, vol. 27, no. 8, pp. 989–999, 2009.

[8] M. Seimetz, "Laser linewidth limitations for optical systems with high-order modulation employing feed forward digital carrier phase estimation," *OFC/NFOEC 2008 - 2008 Conf. Opt. Fiber Commun. Fiber Opt. Eng. Conf.*, pp. 2–4, 2008.

[9] I. Fatadin, D. Ives, and S. J. Savory, "Carrier phase recovery for 16-QAM using QPSK partitioning and sliding window averaging," *IEEE Photonics Technol. Lett.*, vol. 26, no. 9, pp. 854–857, 2014.

[10] G. Goldfarb and G. Li, "BER estimation of QPSK homodyne detection with carrier phase estimation using digital signal processing," *Opt. Express*, vol. 14, no. 18, pp. 8043–8053, Sep. 2006.

[11] W. J. Weber, "Differential Encoding for Multiple Amplitude and Phase Shift Keying Systems," *IEEE Trans. Commun.*, vol. 26, no. 3, pp. 385–391, 1978.

[12] G. Carpintero, E. Rouvalis, K. Ławniczuk, M. Fice, C. C. Renaud, X. J. M. Leijtens, E. a. J. M. Bente, M. Chitoui, F. Van Dijk, and A. J. Seeds, "95 GHz millimeter wave signal generation using an arrayed waveguide grating dual wavelength semiconductor laser," *Opt. Lett.*, vol. 37, no. 17, p. 3657, 2012.

[13] T. Okoschi, K. Kikuchi, and A. Nakayama, "Novel method for high resolution measurement of laser output spectrum," *Electron. Lett.*, vol. 16, no. 16, pp. 630–631, 1980.

[14] K. Balakier, M. J. Fice, F. van Dijk, G. Kervella, G. Carpintero, A. J. Seeds, and C. C. Renaud, "Optical injection locking of monolithically integrated photonic source for generation of high purity signals above 100 GHz," *Opt. Express*, vol. 22, no. 24, p. 29404, 2014.